Interannual to decadal variability in the southern Okhotsk Sea based on a new gridded upper water temperature data set

Shoshiro Minobe[1] and Makoto Nakamura[2]

Division of Earth and Planetary Sciences, Graduate School of Science, Hokkaido University, Sapporo, Japan

Received 15 April 2003; revised 24 March 2004; accepted 23 April 2004; published 8 July 2004.

[1] A new gridded water-temperature data set of upper 200 m depths (0, 50, 100, 200 m depths) for the Okhotsk Sea was produced using an optimal interpolation technique from 1950 to 1996 using oceanographic observations in the World Ocean Database 1998. Temperature variability at 50, 100 and 200 m depths in the southern Okhotsk Sea (south of 52°N) in the warm-season (May–October) was investigated by an Empirical Orthogonal Function (EOF) analysis from 1958 to 1994, for which sufficient data exist for an EOF analysis. The first EOF mode has a monopole structure with the maximal amplitude in the Kuril Basin, and the corresponding Principal Component (PC) exhibits prominent quasi-decadal variability. The first EOF mode is closely related with the wintertime (December–February) sea surface temperature anomalies over the subarctic front or Oyashio front in the North Pacific, and with wintertime Sea level Pressure (SLP) differences between northern Eurasia and the northern North Pacific. This suggests that the temperature changes in the Okhotsk Sea are caused by changes in the strength of the Asian winter monsoon, which are associated with the SLP difference. A quasi-decadal oscillation, similar to that of the PC-1, is observed in the SLP difference since the 1960s, and shared by the Polar/Eurasian (POL) pattern, Arctic Oscillation (AO) and North Atlantic Oscillation (NAO). Some hints of the relating variability are observed in coastal sea level difference between Wakkanai and Abashiri, which was used as a proxy for transport in the Soya Warm Current. Also, some features of sea ice extents co-vary with the PC-1. *INDEX TERMS:* 4215 Oceanography: General: Climate and interannual variability (3309); 4243 Oceanography: General: Marginal and semienclosed seas; 4271 Oceanography: General: Physical and chemical properties of seawater; 4504 Oceanography: Physical: Air/sea interactions (0312); 4540 Oceanography: Physical: Ice mechanics and air/sea/ice exchange processes; *KEYWORDS:* interannual variability, quasi-decadal variability, Okhotsk Sea, sea ice changes, air-sea interaction, climate changes

Citation: Minobe, S., and M. Nakamura (2004), Interannual to decadal variability in the southern Okhotsk Sea based on a new gridded upper water temperature data set, *J. Geophys. Res.*, *109*, C09S05, doi:10.1029/2003JC001916.

1. Introduction

[2] The interannual to decadal variability of the Okhotsk Sea, whose bottom topography and major currents are shown in Figure 1, is an important scientific issue by its own right. Previous studies of this subject have, however, been limited to sea-ice variability since the 1970s. The year-to-year variability of sea-ice extent is known to be influenced by the Siberian High and Aleutian Low, which are the two dominant climatological pressure systems over Eurasia and the North Pacific in winter [*Parkinson*, 1990; *Fang and Wallace*, 1994; *Tachibana et al.*, 1996]. Furthermore, *Ogi et al.* [2004] suggested that the wintertime NAO variability influences the sea-ice extent in April–May.

[3] Changes of water properties in the Okhotsk Sea, however, have hardly been addressed, and the few exceptions were generally based on repeated observations for several years since the 1990s. For example, *Yasuda et al.* [2000] and *Rogachev* [2000a, 2000b] examined hydrographic observations around the Kuril Islands in the early and middle 1990s, and reported that Bussol eddies, which are located just outside of the Okhotsk Sea near the Bussol Strait, are substantially weakened and warmed during this period. However, water property changes in the Okhotsk Sea at periods longer than a decade have not been studied. A long-term analysis, therefore, is important to know the linkage between the oceanographic changes in the Okhotsk Sea and large-scale climate changes, since it is almost impossible to examine such a linkage with reasonable confidence based on short-term (i.e., ten years) data. In order to conduct a long-term analysis, it should be useful to produce a gridded data set, so that one can avoid the

[1] Also at Frontier Research System for Global Change, Yokohama, Japan.

[2] Now at IBM Global Service Japan Solution and Services Company, Sapporo, Japan.

0148-0227/04/2003JC001916$09.00

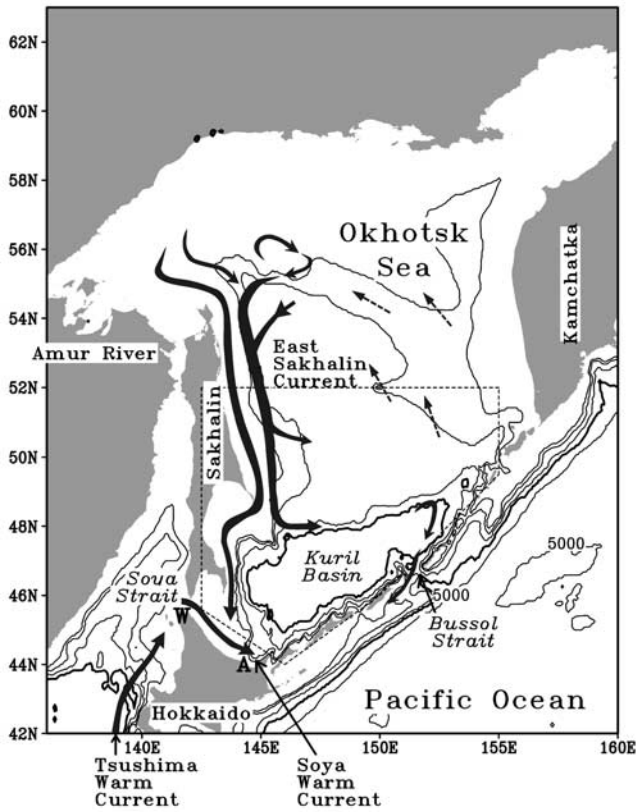

Figure 1. Bottom topography in the Sea of Okhotsk, and schematic of current structures that are important in the southern Okhotsk Sea. The contour levels are 500, 1000, 2000, 3000, and 5000-m depths, with the thick contour for 3000-m depth. The schematic of currents are based on the schematics of *Ohshima et al.* [2002] and Quick Bulletin of Ocean Conditions provided by Hydrographic and Oceanographic Department, Japan Coast Guard (http://www1.kaiho.mlit.go.jp/KAIYO/qboc/index_E.html). The area surronded by a polygon of dashed line indicates the region where the gridded water temperature data have enough coverage for an EOF analysis. Letter W and A indicate the sea level stations at Wakkanai (45°25′N, 141°41′E) and Abashiri (44°01′N, 144°17′E), respectively.

difficulties arising from spatial and temporal irregularity in the distribution of oceanographic observations.

[4] The purpose of the present paper is, therefore, to document interannual to decadal variability of the water temperatures of upper layers in the Okhotsk Sea. For this purpose, we have produced a gridded monthly, 0.5° × 0.5° data set of upper water temperature anomalies of the Okhotsk Sea, using an Optimum Interpolation (OI) method, which has been widely used to produce gridded data sets for the ocean [e.g., *Gandin*, 1963; *White*, 1995]. Number and quality of salinity data are not enough to be gridded reasonably, and hence only temperature data are gridded. Furthermore, although we have processed data in the entire basin of the Okhotsk Sea, sparse observations in the northern Okhotsk Sea prohibit us from obtaining gridded data of reasonable quality for an analysis of interannual to decadal variability in this portion of the basin. Thus we focus our attention on water temperatures in the southern Okhotsk Sea as shown in Figure 1.

[5] It would be useful to summarize major currents in the Okhotsk Sea for the understanding of temperature variations documented in this paper (Figure 1). The strongest current in the southern Okhotsk Sea is the East Sakhalin Current, which consists of two cores, i.e., nearshore core and shelf slope core according to recent float observations [*Ohshima et al.*, 2002]. The East Sakhalin Current provides cold waters from the north, and its transport is estimated as 4–9 Sv (1 Sv = 10^6 m^3 s^{-1}) with the increase from summer to winter [*Ohshima et al.*, 2002]. In contrast, the Soya Warm Current brings warm waters from the Japan Sea. The transports of the Soya Warm Current were observed in the range between 0.5–1.5 Sv from five across-current observations of acoustic Doppler current profiler (ADCP) between 1999 and 2002 off the Hokkaido coast in the Okhotsk Sea [*Tanaka*, 2000]. The Soya Warm Current is known to be stronger in summer than in winter. The Bussol Strait, located to the south of the Kuril Basin, is the main pathway for the subsurface water to flow out from the Okhotsk Sea [*Ohshima et al.*, 2002]. Other general information of the Okhotsk Sea can be seen in the work of *Talley* [2001].

[6] The present paper is organized as follows. Gridding procedures for the oceanographic data, other data including atmospheric data and sea-ice data, and the analysis method are documented in section 2. Interannual to decadal variability of upper layer temperatures in the Okhotsk Sea is described in section 3, and its relation to large-scale atmospheric variations and to sea-ice variations are examined in section 4 and 5, respectively. The summary and discussion are presented in section 6.

2. Data and Analysis Methodology

2.1. Oceanographic Observation Data and Gridding Method

[7] Temperature profiles collected in the CD-ROM version of the World Ocean Database 1998 (WOD1998) [*Levitus et al.*, 1998] are used to produce a gridded temperature data set from 1951 to 1996. The distribution of the observations in each season is shown in Figure 2. There are 19,342 temperature profiles in the Sea of Okhotsk. However, we have excluded the observations near the coast of Hokkaido, where cross-shore temperature gradients are generally greater than 0.1°C km^{-1} in summer due to the Soya Warm Current intruding from the Japan Sea to the Okhotsk Sea [e.g., *Itoh and Ohshima*, 2000]. This exclusion is because we concerned that the climatological temperatures are not correctly obtained in this large gradient region by our method described below. In the case where the climatology is inaccurate, distribution changes of observational locations can result in false temperature anomalies. After removal of these data, the number of temperature profiles was 9182.

[8] Before gridding the data, we applied the following quality control. We first excluded the data that are flagged as erroneous in WOD1998, colder than −2°C, or located at depths deeper than the bottom. Then, we temporarily calculated climatological monthly means at each depth and in each month on a 0.5° × 0.5° degree grid points by a Gaussian filter whose e-folding scale is 100 km. Data more distant than 200 km from the grid point are not used for the climatology calculation. The seasonal cycle is

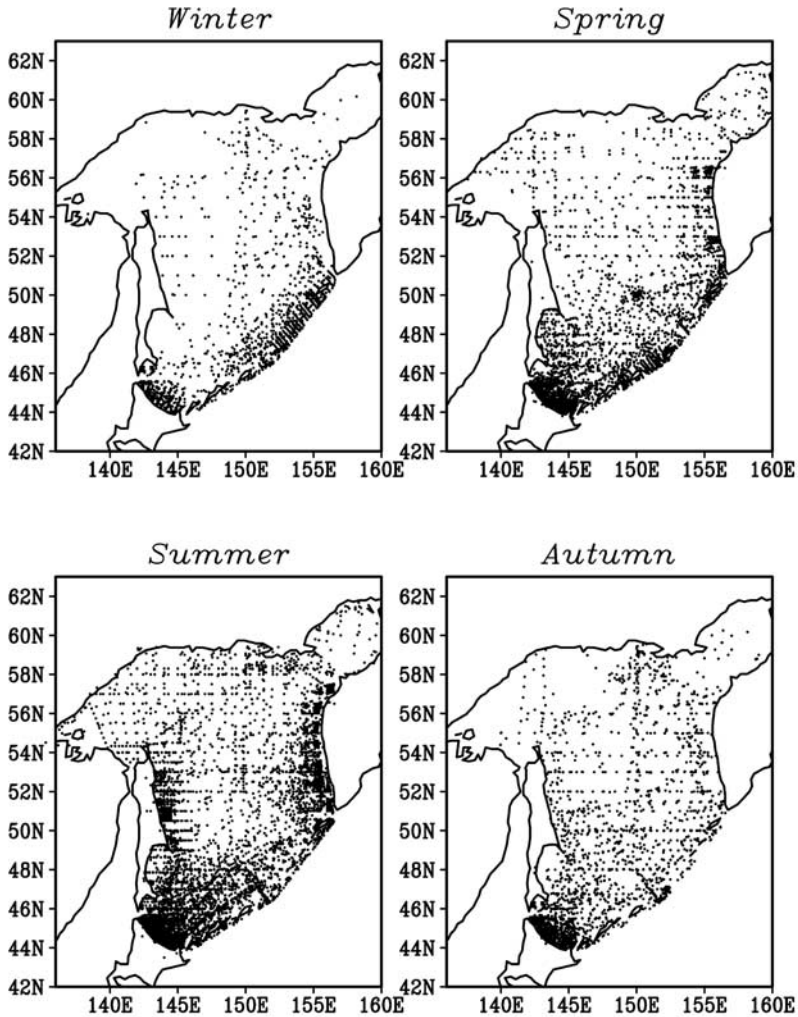

Figure 2. Distribution of observations in winter (December–February), spring (March–May), summer (June–August), and autumn (September–November) during a period from 1950 to 1996.

estimated based on the monthly mean temperatures by fitting to annual and semi-annual cycles in a least squares error sense. The use of the semi-annual cycle in addition to the annual cycle is to represent a seasonal evolution somewhat skewed from a pure sinusoidal wave. For each observation, a climatological temperature is estimated from the fitted climatology, and an anomaly is defined as the difference of the observed temperature from the climatology. A datum whose anomaly is larger than 2.5 times of the standard deviation of anomalies at the corresponding grid point is removed from further analyses. This quality control scheme removes 4.0% of the surface data and 5.0% at 200-m depth. After removing these data, the monthly climatology and observed temperature anomalies from the climatology are re-calculated using the same method as described above.

[9] We employ an optimal interpolation (OI) technique to produce the gridded water temperature anomalies on a monthly, $0.5^\circ \times 0.5^\circ$ grid at four levels of 0, 50, 100, and 200-m depths. In an OI, observed data are assumed to be a superposition of signal and noise, and the estimated signal values are gridded. Before gridding, the spatiotemporal structure of the signal, which is expressed by autocorrelation functions, and signal-to-noise ratios should be estimated.

[10] A signal-to-noise ratio, defined as a square root of the ratio of the signal variance to the noise variance, is estimated from anomaly temperatures at each depth as follows. We calculated signal variance by averaging covariance for all pairs of individual observations separated by less than 50 km in the same month and year. Here, we have assumed that a lag smaller than 50 km and one month can be ignored for a signal. The covariance here does not include auto-covariance, i.e., the covariance is calculated from only the pairs of two different observations. On the other hand, auto-covariance gives the total (signal plus noise) variance. Thus we obtained the noise variance by subtracting the signal variance from the total variance. Observed signal-to-noise ratios from the surface to the 200-m depth are summarized in Table 1.

[11] For the estimation of the autocorrelation functions for the signal and subsequent gridding, we use so-called *super observations* [*White*, 1995]. A super observation is a substitutional datum representing raw anomalies over a

Table 1. Parameters Used for Optimum Interpolation Gridding[a]

Depth	S/N	D_x	D_y	D_t
0 m	0.7	5.5	3.6	0.94
50 m	1.2	2.5	1.7	1.8
100 m	1.1	2.0	2.4	2.5
200 m	1.4	2.5	3.0	6.5

[a]S/N is the signal-to-noise ratio, D_x and D_y are the zonal and meridional decorrelation scales in units of degree (longitude and latitude), respectively, and D_t is the temporal decorrelation scale in units of month.

$0.5° \times 0.5°$ bin in a month and in a year at each depth. The value of the super observation is given by the average of raw anomalies in the bin, and location is defined at the position of the gravity center of the raw observations. The use of the super observations significantly reduces the computation amount and also the complexity of program coding.

[12] In the present OI, the autocorrelation function for the signal is assumed to have a Gaussian form as,

$$r(d_x, d_y, d_t) = \exp\left(-(d_x/D_x)^2 - (d_y/D_y)^2 - (d_t/D_t)^2\right) \quad (1)$$

where r is the autocorrelation function, d_x and d_y are the zonal and meridional distances, respectively, d_t is the temporal differences, and D_x, D_y and D_t are the respective decorrelation scales. The decorrelation scales are estimated by fitting equation (1) to observed autocorrelations, which are calculated using the super observations. The spatial decorrelation scales at depth are much smaller than those at the surface, while the opposite tendency is found for the temporal scales (Table 1).

[13] The gridded temperature anomalies are estimated from the super observations with the OI parameters by a standard OI method as described by *White* [1995] in detail. In the case where there is no observation within the e-folding temporal and spatial distance from the center of a grid, the gridded anomaly is treated as unavailable. After the gridded anomalies are calculated by the OI, the climatology and anomaly fields are re-calculated.

[14] Given the fact that there are no abundant observations in the Okhotsk Sea especially in winter season (Figure 2), we averaged the gridded water temperature anomalies over the warm-season (May–October) in each year, yielding annually sampled anomaly data, which are used in the following analyses. We assume that the warm-season subsurface temperature anomalies may hold information of wintertime atmospheric forcings, isolated from summertime atmospheric forcing by a shallow mixed layer,

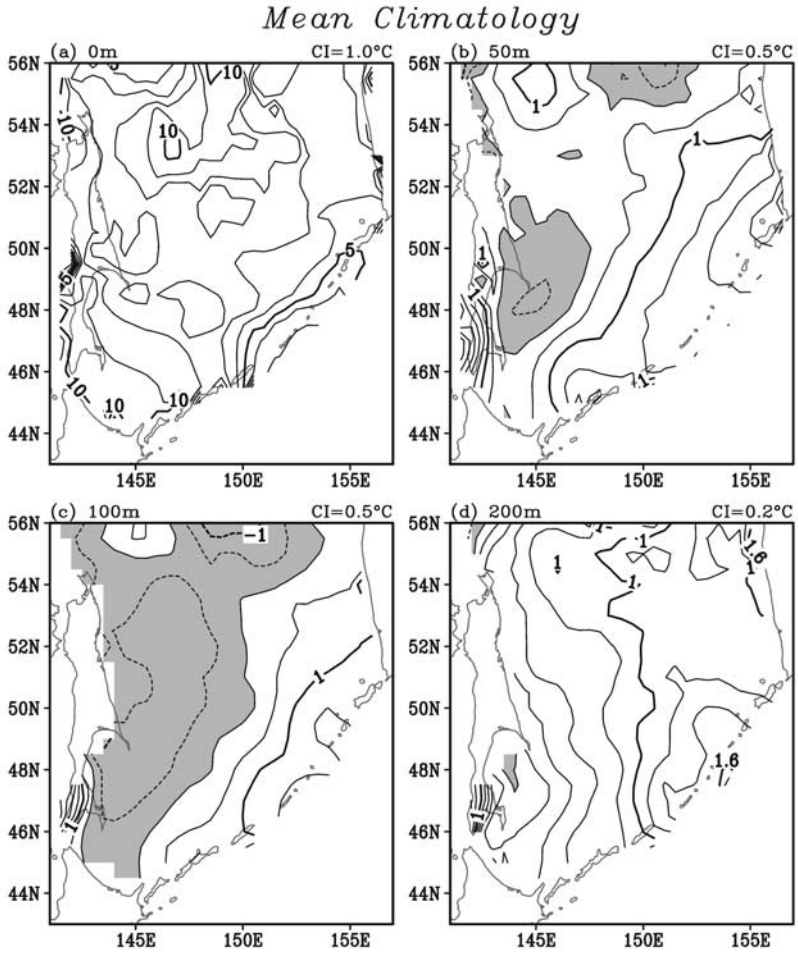

Figure 3. Summer-mean (May–October) climatological temperature in the Okhotsk Sea at 0, 50, 100, and 200 m depths. Contour intervals are 1.0, 0.5, 0.5, and 0.2°C, at 0, 50, 100, and 200 m depths, respectively. Shading indicates the regions where temperatures are less than zero.

consistent with *Wakatsuchi and Martin* [1990]. The winter mixed layer can be as deep as 300 m depth as observed in 1997 [*Ohshima*, 2001]. As will be shown later, this assumption is likely to be the case, because a significant and well-organized structure of the wintertime atmospheric circulation anomalies accompanies the sub-surface temperature anomalies in warm-season.

[15] Figure 3 shows fitted climatological temperature averaged over the warm-season (May–October) at 0, 50, 100, and 200 m depths. At the sea surface, temperature maxima occur over the Hokkaido coast and minima over the northern Kuril Islands. On the other hand, at 50, 100, and 200 m depths temperature maxima occur over the eastern part of the Okhotsk Sea and minima over the western part. A noticable feature of the climatology is the fact that the water temperature at 50 and 100 m depths is below 0°C over the northwestern part, indicating a dicho-thermal layer. The temperature distribution is consistent with a previous study of climatology by *Watanabe and Wakatsuchi* [1998].

2.2. Additional Data

[16] In order to understand the relations between the upper layer temperature changes in the Okhotsk Sea and other physical environmental variations, we examine the following data in the present study. Monthly 5° × 5° Sea Level Pressure (SLP) in the northern hemisphere, which is an updated version of the SLP data of *Trenberth and Paolino* [1980], was obtained from the National Center for Atmospheric Research (NCAR) Data Support Section. Monthly wind speeds at 1000 hPa height on a 2.5° × 2.5° grid and Surface Temperatures (STs) (SSTs over the ocean and land surface temperatures otherwise) on a Gaussian grid (1.85° in longitude and about 1.9° in latitude around the Okhotsk Sea) are obtained from the National Centers for Environmental Prediction (NCEP) – NCAR reanalysis from 1949 to 2002 [*Kalnay et al.*, 1996].

[17] We also use teleconnection pattern indices and Arctic Oscillation index. The teleconnection indices for Polar/Eurasia pattern (POL), North Atlantic Oscillation (NAO) and others are obtained as leading modes of a rotated EOF analysis of the 700-mb height fields by the Climate Prediction Center (CPC) [*Bell and Halpert*, 1995], and index of Arctic Oscillation (AO), which is the first mode of the EOF analysis of SLP north of 20°N [*Thompson and Wallace*, 1998], is also provided from CPC. The first mode in the rotated EOF analysis was POL from December to February, and is similar to the 500-mb height regression map of the AO.

[18] In addition to these atmospheric data, we also examine a time series for sea level displacement (SLD) difference between Wakkanai and Abashiri (Wakkanai minus Abashiri) and a time series for sea-ice extension (SIE) of the Okhotsk Sea. Sea level data at Wakkanai (45°25′N, 141°41′E) and Abashiri (44°01′N, 144°17′E) are obtained from Japan Oceanographic Data Center from 1968 to 2001, and annual mean differences between them are calculated. Figure 1 shows the locations of these stations. This SLD difference is known to represent well transport changes of the Soya Warm Current at the Soya Strait; the correlation between the SLD difference and the strait transport is as high as 0.76 using the data of eleven trans-strait ADCP observations from 1996 to 1999 [*Tanaka*, 2000]. This relation is consistent with the fact that the primary cause of the Soya Current is the sea level difference between the Okhotsk Sea and the Japan Sea [*Ohshima*, 1994]. The SIE data was provided from Japan Meteorological Agency (JMA) from 1971 to 2000. The data are provided as a CD-ROM titled "The statistical data of sea ice Vol. 3 (Period: 1971–2000)." The SIE data are estimated from various sources of observations including visual inspections, air-craft observations and satellite observations.

2.3. Methodology of Analysis

[19] In order to extract dominant modes in water temperatures in upper layers of the Okhotsk Sea, Empirical Orthogonal Function (EOF) analysis is applied to the aforementioned warm-season (May–October) averaged temperatures at 50, 100 and 200 m depths combined, based on a covariance matrix. The EOFs are calculated with data from 1958–94 in order to avoid data gaps. Because of a number of gaps in the temperature data set at 50–200 m depths in the northern Okhotsk Sea, our analysis area is limited to the southern Okhotsk Sea (south of 52°N, see Figure 1). In order to extract the relationship between the ocean and atmosphere or sea-ice, we calculated correlation coefficients between the Sea Level Pressures (SLPs) and Sea-Ice Extent (SIE) onto the Principal Component (PC) or time coefficient of the EOFs. If we assume that data in each year are independent, a correlation coefficient larger than 0.33 is significant at the 95% confidence level. However, data from each year may not be independent, reflecting quasi-decadal variability observed in the Okhotsk Sea as shown in the next section. Thus we also examine coherency, since coherency is the most relevant tool to examine the relation of two variables on a specific timescale.

3. Water Temperature Variability

[20] The first EOF mode for warm-season water temperature anomalies at 50, 100 and 200 m depths combined explains 36% of the total variance. The explained variances of the 2nd and 3rd modes are 14% and 10%, respectively. Not only because of the small-explained variance of the 2nd and 3rd modes and their small difference, but also because atmospheric circulation anomalies for these modes are not well-organized, we suppose that these two modes may not be physically meaningful. Thus we focus on the first mode in the present paper.

[21] Figure 4 shows the spatial structure and temporal coefficient of the first EOF mode. The regression and correlation coefficients exhibit a monopole structure at 50 and 100 m depths with stronger amplitudes than at 200 m depth, and at these upper two levels the center of the pattern is located in the Kuril Basin (Figures 4a–4c). The PC-1 is characterized by four prominent peaks that roughly occur at ten-year intervals, indicating the occurrence of quasi-decadal variability (Figure 4d). *Wakatsuchi and Martin* [1990] showed that subsurface waters of the Kuril Basin in summer 1979 were coldest from 1978 to 1982, consistent with a negative peak of the PC-1.

[22] The quasi-decadal variability in PC-1 resembles the decadal variability of the subarctic front in the North Pacific reported by *Nakamura et al.* [1997] (see their Figure 3a). The correlation map between the wintertime (December–Febru-

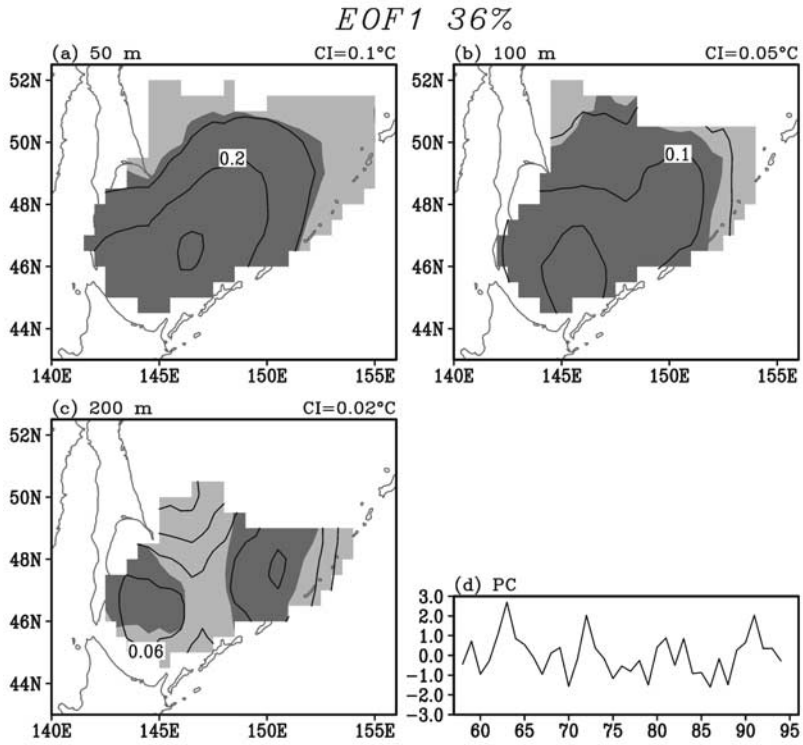

Figure 4. (panels a–c) Spatial pattern of the first EOF mode of warm-season water temperatures at 50, 100 and 200 m depths combined. The contours indicate the regression coefficients of the temperatures onto the PC-1, and shading indicates grids based on which EOFs are calculated, with dense shade indicating the correlation coefficients larger than 0.4. The maximal correlations are 0.86, 0.81, and 0.52 at 50, 100 and 200 m depths, respectively. (panel d) The corresponding time coefficient or the first Principal Component (PC-1).

ary) STs and PC-1 confirms this resemblance, because high-correlations penetrate from the western end of the North Pacific toward the east between 40° and 50°N (Figure 5). Thus the first EOF mode of the Okhotsk Sea is most likely to be related to the large-scale variability of the atmosphere and ocean. Although the quasi-decadal variability is common between the Okhotsk Sea and the North Pacific, the 1970s climate regime shift, which is prominent in the North Pacific subarctic front [*Nakamura et al.*, 1997] is not apparent in the PC-1 for the Okhotsk Sea. The 1970s shift is one of three major climate regime shifts in the 20th century along with the other shifts in the 1920s and 1940s [*Minobe*, 1997]. The reason why the 20–30-yr long regimes occurred is not yet known, but the rapidity of the transition between the regimes is hypothesized as a resonance between 20-yr and 50–70-yr oscillations [*Minobe*, 1999, 2000]. Furthermore, it is noteworthy that the PC-1 does not show any evidence for the 20-yr oscillation, which is quite prominent in the Aleutian low variability [e.g., *Minobe et al.*, 2002].

[23] Is the first EOF mode related to circulation anomalies in the Okhotsk Sea? Here we examine the sea level difference between Wakkanai and Abashiri, which represents the Soya Warm Current transports as noted in section 2. The sea level difference shown in Figure 6 exhibits decadal co-variability with the PC-1. The peak in the early 1990s in sea level difference is much larger than the peaks in the early 1980s and early 1970s, though the three corresponding peaks of the PC-1 show similar magnitudes. Quasi-decadal variability similar to that of the Okhotsk PC-1 was also observed in the northern Japan Sea [*Minobe et al.*, 2004], and hence not only the variability of the Okhotsk

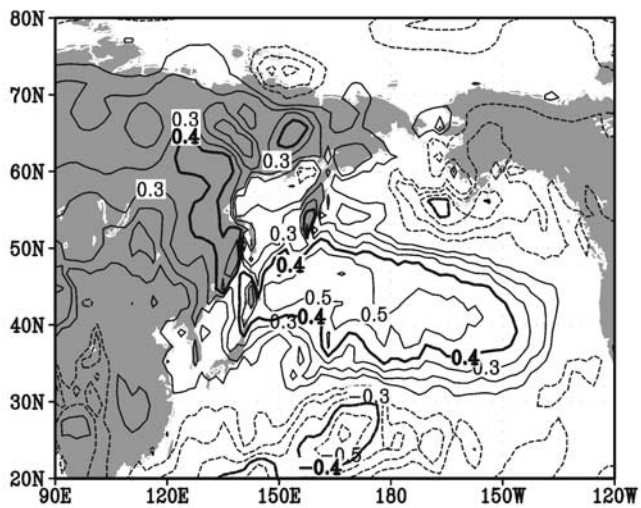

Figure 5. Correlation coefficients of wintertime Surface Temperatures (STs) (SSTs over the ocean and land surface temperatures otherwise) onto the PC-1 shown in Figure 4d. Contour interval is 0.1 without zero contours, and thick contour indicates ±0.4.

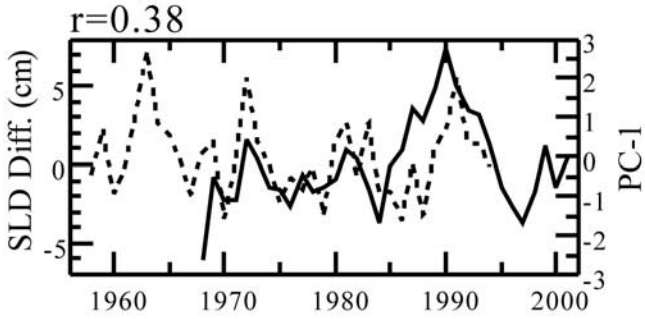

Figure 6. Sea level difference, Wakkanai minus Abashiri, (solid line, left axis) and PC-1 shown in Figure 4d (dashed line, right axis). Correlation coefficient between them is 0.38.

Sea, but the variability of the Japan Sea may be responsible for the transport changes of the Soya Warm Current.

4. Atmospheric Circulation Variability

[24] We assume that the subsurface water temperature in the southern Okhotsk Sea retains the information of atmospheric forcing from the previous winter, following the study of *Wakatsuchi and Martin* [1990], who showed that wintertime cooling over the Kuril Basin played a dominant role in summertime subsurface water temperatures. It is noteworthy, however, a recent float observation showed that water masses in the northwestern region of the Okhotsk Sea flow out to the Pacific Ocean through the Kuril Basin within a half year [*Ohshima et al.*, 2002]. This suggests that a significant portion of warm-season waters in the Kuril Basin were possibly located in the previous winter in upstream region given the counter-clockwise general circulation of the Okhotsk Sea [*Shimizu and Ohshima*, 2002; *Ohshima et al.*, 2002] (Figure 1), and hence the region where the wintertime atmospheric cooling is important in the waters in the Kuril Basin in the following warm-season may not be the Kuril Basin but elsewhere in the Okhotsk Sea. Thus rather than examining the atmospheric forcing only over the Kuril Basin, we focus on large-scale atmospheric changes corresponding to the oceanographic changes.

[25] Figure 7 shows that wintertime (December–February) SLPs have large negative correlations with the PC-1 over northern Eurasia and large positive correlations over the northern North Pacific. The former region has smaller (larger) absolute correlations than the latter, when correlations are calculated using the data without (with) a 7-yr low-pass filtering. We compare the PC-1 with a SLP difference time series, which is given by SLPs averaged over the northern North Pacific minus SLPs averaged over northern Eurasia (Figure 8). The covariability between the PC-1 and SLP difference is prominent with the correlation coefficient as high as 0.49. This covariability is mainly due to decadal-scale variability (Figure 9), and is almost absent in high-pass (period < 7-yrs) filtered time series with the correlation as low as 0.20 (insignificant at the 80% confidence limit).

[26] A coherency analysis further confirms that the statistically significant relation between the PC-1 and the SLP difference between the northern North Pacific and northern Eurasia (Figure 10). The coherency is remarkably high on the decadal period, and is significant at the 99% confidence limit. Moreover, the SLP time series averaged over the northern North Pacific or over northern Eurasia has 1% significant quasi-decadal coherency peak with the PC-1, with a 180° out-of-phase relation between the two SLP time series (not shown). Consequently, the out-of-phase SLP variability over the northern North Pacific and northern Eurasia, which effectively influences the Asian winter

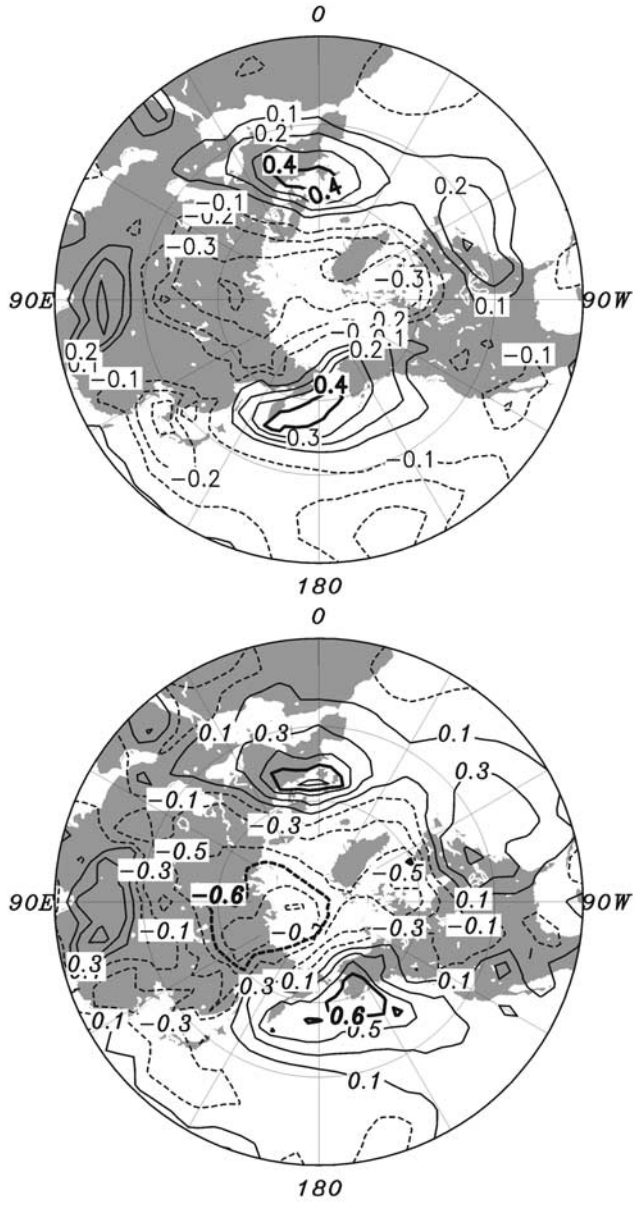

Figure 7. Correlation coefficients of wintertime SLPs onto the PC-1 shown in Figure 4d without temporal filtering (upper panel) and with a 7-yr low-pass filtering (lower panel) in a north polar stereographic map north of 20°N. For the upper panel, contour interval is 0.1 without zero contours, and for the lower panel the contour interval is 0.1 (0.2) for absolute correlations smaller (larger) than 0.5. Thick contours indicate ±0.4 and ±0.6 in the upper and lower panels, respectively.

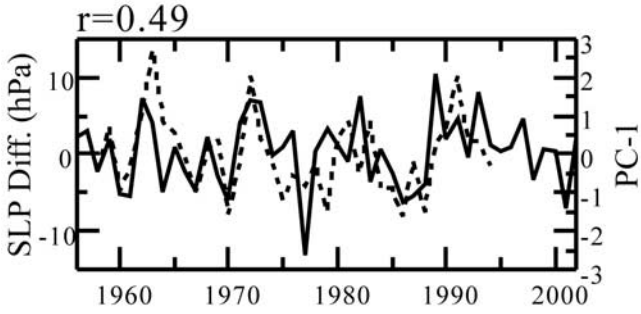

Figure 8. Same as Figure 6, but for wintertime SLP difference, which is defined by SLP averaged over the northern North Pacific (50°–60°N, 160°E–140°W) minus SLP averaged over northern Eurasia (50°–80°N, 50°–130°E). The correlation coefficient between the two time series is 0.49.

monsoon, is closely related with the PC-1 on the quasi-decadal timescale.

[27] The regression coefficients of the zonal and meridional wind speeds at 1000 hPa height in winter season onto the PC-1 indicate that, when subsurface Okhotsk Sea is warm, the easterly and southeasterly wind anomalies prevails over the southern and northern Okhotsk Sea, respectively (Figure 11), consistent with the SLP changes. These wind anomalies bring warm and moist air from the North Pacific to Eurasia, and warm the Okhotsk Sea via sensible and latent heat fluxes between the atmosphere and the ocean.

[28] These results suggest that a stronger East Asian winter monsoon, related with both the stronger Siberian highs and Aleutian lows, cools subsurface temperatures in the southern Okhotsk Sea on the quasi-decadal timescale. The temperature variability in the northern Japan Sea also exhibited decadal co-variability with the SLP changes over the northern part of the Siberian highs [*Minobe et al.*, 2004].

[29] The SLP correlation maps with the PC-1 shown in Figure 7 indicate hemispheric structures, suggesting that the Okhotsk Sea temperature variations related with some teleconnection patterns. Thus we calculate the correlations between the teleconnection pattern indices of CPC and the PC-1. The gravest correlation (r = 0.36) is found for the POL pattern followed by the Western Pacific (WP) pattern (r = −0.33). The distributions of the regression coefficients

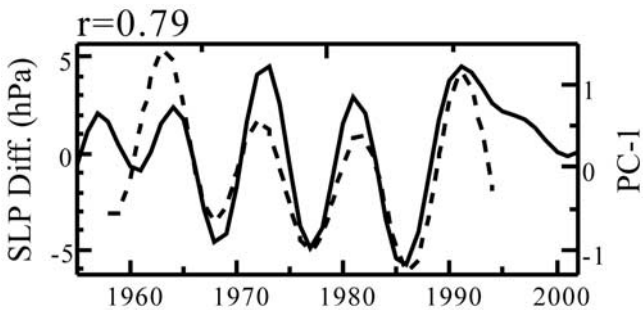

Figure 9. Same as Figure 8, but for time series smoothed by a 7-yr low-pass filtering. The correlation coefficient between the two time series is 0.79.

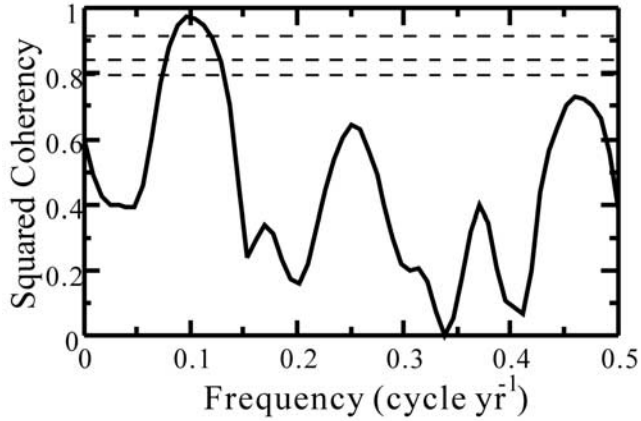

Figure 10. Squared coherency between the PC-1 and SLP difference between the northern North Pacific (50°–65°N, 160°E–140°W) and northern Eurasia (50°–80°N, 50°–130°E). The horizontal dashed lines indicate the confidence levels at 95, 97 and 99%.

of winter SLPs onto the winter POL index resembles the correlation map for the PC-1 over Eurasia, the Arctic and the Atlantic, but the strong correlations over the northern North Pacific observed in the correlation map with the PC-1 are absent in the wintertime SLP structure of POL (not shown).

[30] The highest coherency for the teleconnection indices with the PC-1 is found for POL on the quasi-decadal timescale (significant at the 97% confidence limit), consistent with the aforementioned highest correlation between the POL and PC-1 (not shown). Furthermore, the AO and North Atlantic Oscillation (NAO) exhibit a significant quasi-decadal coherency peak with the PC-1 at the 95% and 90% confidence limits, respectively. A time series comparison indicates that these indices share a

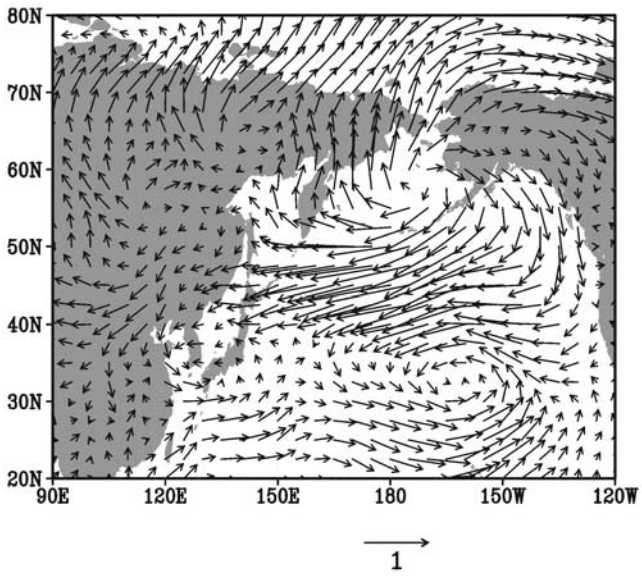

Figure 11. Regression coefficients of wintertime wind speeds at 1000 hPa onto the PC-1 shown in Figure 4d. Reference arrow indicates 1 m s^{-1}.

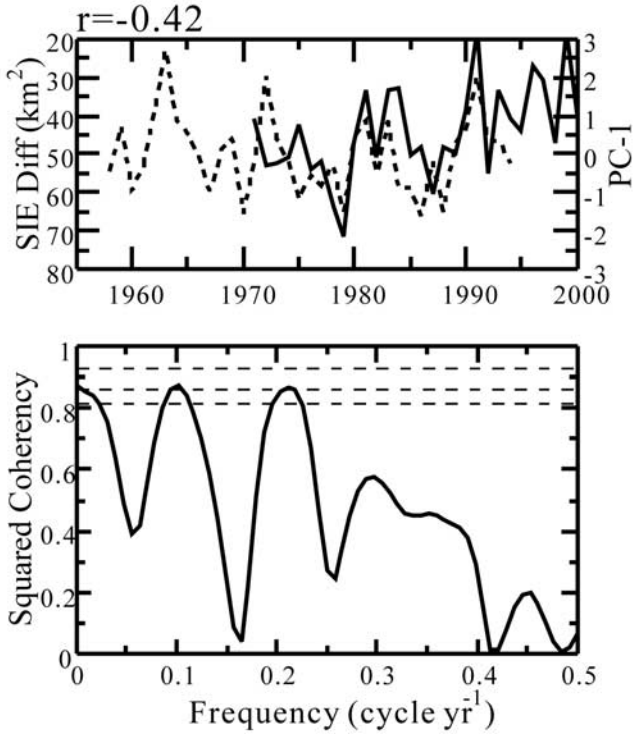

Figure 12. (top panel) January minus December Sea-Ice Extent (SIE) difference (solid line, left axis) and the PC-1 shown in Figure 4d (dashed line, right axis). It is noteworthy that the left axis is reversed, and hence warmer (colder) water temperatures correspond to slower (faster) SIE advances. (bottom panel) Coherency between the SIE difference and the PC-1. The horizontal dashed lines indicate the confidence levels at 95, 97 and 99%.

quasi-decadal variability from 1970 (not shown). Although it is subject of debate whether the Arctic Oscillation is a physically meaningful mode [*Wallace and Thompson*, 2002] or an artifact [*Deser*, 2000], it is important to note that the POL, AO and NAO are associated with the prominent quasi-decadal variability of the Okhotsk Sea temperatures. The WP pattern, which exhibited higher correlations with the PC-1 than the AO and NAO as mentioned above, does not have a significant peak on decadal-interdecadal timescales.

5. Sea-Ice Extent Variability

[31] As described in section 1, most previous studies of interannual and decadal variability in the Okhotsk Sea addressed sea-ice variations. Thus it is interesting to examine whether or not the temperature variability in the Okhotsk Sea, which is related to the hemispheric-scale circulation anomalies of the atmosphere, is commonly found in sea-ice field. To answer this question, we examined sea-ice extent (SIE) data available since 1971.

[32] The correlation coefficients of SIEs in each month with the PC-1 are 0.03 (December), −0.29 (January), −0.11 (February), −0.19 (March), −0.13 (April), and −0.40 (May). The absolute value of correlation coefficients are generally smaller than 0.3, though correlation of 0.41 (0.35) is required to be significant at the 95% (90%) confidence level in this case. Relatively high-correlations are observed in May (−0.40). However, coherency analysis shows that there is no significant decadal peak between the PC-1 and SIE in May, but a 95% significant decadal peak occurs between the PC-1 and SIE in January (not shown).

[33] We further examined the relation between the SIE differences between successive two months. The SIE difference represents the speeds at which the sea-ice advances or retreats. The highest correlation is found between the PC-1 and the SIE difference between January and December (r = −0.43), with absolute correlations for other months being less than 0.3. Time series comparison shows prominent co-variability between the PC-1 and SIE, accompanied by a 97% significant coherency peak on the decadal timescale (Figure 12). The good relation between the PC-1 and the sea-ice advance, which may be primarily due to ice-advection by winds [*Kimura and Wakatsuchi*, 1999], between January and December suggest that the anomalous sea-ice advance is an aspect of the coherent changes of the Okhotsk Sea and adjacent atmospheric circulation anomalies in the early winter. *Wakatsuchi and Martin* [1990] demonstrated anomalous atmospheric cooling over Kuril Basin occurred in early winter (December and January), i.e., before sea-ice expanded over the basin.

6. Summary and Discussion

[34] In the present study, upper water temperature anomalies using a newly produced temperature data set in the southern Okhotsk Sea is examined by an EOF analysis. The EOF analysis is performed for warm-season (May–October) water temperature anomalies in the southern Okhotsk Sea from 1958 to 1994. This is the first attempt to describe the water property changes in the Okhotsk sea for a period longer than a decade. The first EOF mode has large amplitudes in the Kuril Basin, and its temporal variability exhibits the quasi-decadal variability. This mode is highly correlated with the wintertime SST anomalies over the subarctic front or Oyashio front in the North Pacific, and with the SLP difference between northern Eurasia and the northern North Pacific. The spatial pattern of the correlations of the wintertime SLPs onto the PC-1 somewhat resembles the correlations of SLP with the POL index, but the wintertime POL does not have strong correlations over the northern North Pacific. The quasi-decadal variability in the PC-1 is shared by the POL as well as AO and NAO. This may mean that the quasi-decadal variability of the POL, AO and NAO influences the Okhotsk Sea by changing the East Asian winter monsoon associated with changes in the northern parts of the Siberian high and Aleutian low. Given the recent observational result that water masses in the northwestern region of the Okhotsk Sea flow out to the Pacific Ocean through the Kuril Basin within a half year [*Ohshima et al.*, 2002], the temperature changes in the southern Okhotsk Sea probably reflect the changes of the upstream region. The relation between the stronger (weaker) Asian winter monsoons with the colder (warmer) Okhotsk Sea temperatures suggests that the atmospheric thermal forcings, i.e., warming and cooling, of upstream waters play an important role. The transport changes of the Soya Warm Current, SIE changes in May, and fluctuations of SIE advance in December and January

are closely related with the PC-1 and hence can be regarded as different aspects of a single, well-organized variability in the Okhotsk Sea.

[35] It is interesting to note that *Yasuda et al.* [2000] and *Rogachev* [2000a, 2000b] reported that Bussol eddies, which are located just south of the Bussol Strait, substantially changed their properties from a colder and fresher state to a warmer and more saline state from 1990 to 1996. During this period, the present study showed that the subsurface water temperature in the southern Okhotsk Sea exhibited a decreasing trend (Figure 4), and the SLP differences between the northern North Pacific and northern Eurasia shown in Figures 8 and 9 also exhibit a consistent trend, suggesting that the Asian winter monsoon became more stringent. Such trend-like changes inside and just outside of the Okhotsk Sea suggest that there might be a relationship between them, and the present results showed that similar changes in the Okhotsk Sea occurred on the decadal timescale also before 1990. Such changes in the Okhotsk Sea and just outside of it may influence water and circulation properties in a wider area of the North Pacific. For example, a source water of the North Pacific Intermediate Water, which is formed by mixing of saline Kuroshio waters and fresh Oyashio waters [*Talley et al.*, 1995; *Yasuda et al.*, 1996], comes from the Okhotsk Sea [*Yasuda*, 1997]. To understand the role of the Okhotsk Sea in climate variability on interannual to decadal timescales requires further numerical and observational studies.

[36] **Acknowledgments.** We thank M. Wakatsuchi for encouragements on this study, L. Talley, S. Riser, I. Yasuda and for invaluable discussions, S. Martin, K. I. Ohshima for their help as editors for the special issue, and anonymous reviewers for their constructive comments. Some figures are produced with the GrADS package developed by B. Doty. This study is supported by a fund from Core Research for Evolution Science and Technology (CREST), Japan Science and Technology Corporation (JST), by a grant from the Japanese Ministry of Education, Culture, Sports, Science and Technology, and by 21st century center of excellence program on "Neo-Science of Natural History" lead by H. Okada from the Ministry of Education, Culture, Sports, Science and Technology, Japan.

References

Bell, G. D., and M. S. Halpert (1995), Atlas of intraseasonal and interannual variability, 1986–1993. NOAA Atlas No. 12. Climate Prediction Center, NOAA/NWS/NMC, Washington D.C.

Deser, C. (2000), On the teleconnectivity of the "Arctic Oscillation," *Geophys. Res. Lett.*, *27*, 779–782.

Fang, Z., and J. M. Wallace (1994), Arctic sea ice variability on a timescale of weeks and its relation to atmospheric forcing, *J. Clim.*, *7*, 897–1914.

Gandin, L. S. (1963), *Objective Analysis of Meteorological Fields*, 266 pp., Gidro-Meteorizdat, Leningrad, Russia.

Itoh, M., and K. I. Ohshima (2000), Seasonal variations of water masses and sea level in the southwestern part of the Okhotsk Sea, *J. Oceanogr.*, *56*, 643–654.

Kalnay, E., et al. (1996), The NCEP/NCAR 40-year reanalysis project, *Bull. Am. Meteorol. Soc.*, *77*, 437–472.

Kimura, N., and M. Wakatsuchi (1999), Processes controlling the advance and retreat of sea ice in the Sea of Okhotsk, *J. Geophys. Res.*, *104*, 11,137–11,150.

Levitus, S., T. P. Boyer, M. E. Conkright, T. O'Brien, J. Antonov, C. Stephens, L. Stathoplos, D. Johnson, and R. Gelfeld (1998), *World Ocean Database 1998* vol. 1, *Introduction, NOAA Atlas NESDIS 18*, Natl. Oceanic and Atmos. Admin., Silver Spring, Md.

Minobe, S. (1997), A 50–70 year climatic oscillation over the North Pacific and North America, *Geophys. Res. Lett.*, *24*, 683–686.

Minobe, S. (1999), Resonance in bidecadal and pentadecadal climate oscillations over the North Pacific: Role in climatic regime shifts, *Geophys. Res. Lett.*, *26*, 855–858.

Minobe, S. (2000), Spatio-temporal structure of the pentadecadal variability over the North Pacific, *Prog. Oceanogr.*, *47*, 99–102.

Minobe, S., T. Manabe, and A. Shouji (2002), Maximal wavelet filter and its application to bidecadal oscillation over the Northern Hemisphere through the 20th century, *J. Clim.*, *15*, 1064–1075.

Minobe, S., A. Sako, and M. Nakamura (2004), Interannual to interdecadal variability in the Japan Sea based on a new gridded upper water temperature data set, *J. Phys. Oceanogr.*, in press.

Nakamura, H., G. Lin, and T. Yamagata (1997), Decadal climate variability in the North Pacific during the recent decades, *Bull. Am. Meteorol. Soc.*, *78*, 2215–2225.

Ogi, M., Y. Tachibana, and K. Yamazaki (2004), The connectivity of the Okhotsk sea ice with the Okhotsk high and their relation to the winter North Atlantic Oscillation (NAO), *J. Meteorol. Soc. Jpn.*, in press.

Ohshima, K. I. (1994), The flow system in the Japan Sea caused by a seal level difference through shallow straits, *J. Geophys. Res.*, *99*, 9925–9940.

Ohshima, K. I. (2001), Winter oceanographic conditions in the southwestern part of the Okhotsk Sea and their relation to sea ice, *J. Oceanogr.*, *57*, 451–460.

Ohshima, K. I., M. Wakatsuchi, Y. Fukamachi, and M. Genta (2002), Near-surface circulation and tidal currents of the Okhotsk Sea observed with satellite-tracked drifters, *J. Geophys. Res.*, *107*(C11), 3195, doi:10.1029/2001JC001005.

Parkinson, C. L. (1990), The impact of the Biberian High and Aleutian Low on the sea-ice cover of the Sea of Okhotsk, *Ann. Glaciol.*, *14*, 226–229.

Rogachev, K. A. (2000a), Rapid thermohaline transition in the Pacific western subarctic and Oyashio fresh core eddies, *J. Geophys. Res.*, *105*, 8513–8526.

Rogachev, K. A. (2000b), Recent variability in the Pacific western subarctic boundary currents and Sea of Okhotsk, *Prog. Oceanogr.*, *47*, 299–336.

Shimizu, D., and K. I. Ohshima (2002), Barotropic response of the Sea of Okhotsk to wind forcing, *J. Oceanogr.*, *58*, 851–860.

Tachibana, Y., M. Honda, and K. Takeuchi (1996), The Abrupt decrease of the sea ice over the Southern part of the Sea of Okhotsk in 1989 and its relation to the recent weakening of the Aleutian Low, *J. Meteorol. Soc. Jpn.*, *74*, 579–584.

Talley, L. D. (2001), Okhotsk Sea circulation, *Encyclopedia of Ocean Sciences*, vol. 4, edited by J. H. Steele, K. K. Turekian, and S. A. Thorpe, pp. 2007–2015, Academic, San Diego, Calif.

Talley, L. D., Y. Nagata, M. Fujimura, T. Iwao, T. Kono, D. Inagake, M. Hirai, and K. Okuda (1995), North Pacific intermediate water in the Kuroshioo/Oyashio mixed water region, *J. Phys. Oceanogr.*, *25*, 475–501.

Tanaka, I. (2000), A method to estimate residual volume transport of the Soya Warm Current, paper presented at 15th International Symposium on Okhotsk Sea and Sea Ice, Okhotsk Sea and Cold Ocean Res. Assoc., Mombetsu, Japan.

Thompson, D. W. J., and J. M. Wallace (1998), The Arctic Oscillation signature in the wintertime geopotential height and temperature fields, *Geophys. Res. Lett.*, *29*, 1297–1300.

Trenberth, K. E., and D. A. Paolino (1980), The Northern Hemisphere sea-level pressure data set: Trends, errors and discontinuities, *Mon. Weather Rev.*, *108*, 855–872.

Wakatsuchi, M., and S. Martin (1990), Satellite-observations of the ice cover of the Kuril basin region of the Okhotsk Sea and its relation to the regional oceanography, *J. Geophys. Res.*, *95*, 13,393–13,410.

Wallace, J. M., and D. W. Thompson (2002), The Pacific center of action of the Northern Hemisphere annular mode: Real or artifact?, *J. Clim.*, *15*, 1987–1991.

Watanabe, T., and M. Wakatsuchi (1998), Formation of 26.8–26.9 σ_θ water in the Kuril Basin of the Sea of Okhotsk as a possible origin of North Pacific Intermediate Water, *J. Geophys. Res.*, *103*, 2849–2865.

White, W. B. (1995), Design of a global observing system for gyre-scale upper ocean temperature variability, *Prog. Oceanogr.*, *36*, 169–217.

Yasuda, I. (1997), The origin of the North Pacific Intermediate Water, *J. Geophys. Res.*, *102*, 893–909.

Yasuda, I., K. Okuda, and Y. Shimizu (1996), Distribution and modification of North Pacific Intermediate Water in the Kuroshio-Oyashio interfrontal zone, *J. Phys. Oceanogr.*, *26*, 448–465.

Yasuda, I., S.-I. Ito, Y. Shimizu, K. Ichikawa, K.-I. Ueda, T. Honma, M. Uchiyama, K. Watanabe, N. Sunou, K. Tanaka, and K. Koizumi (2000), Cold-core anticyclonic eddies south of Bussol' Strait in the northwestern Subarctic Pacific, *J. Phys. Oceanogr.*, *30*, 1137–1157.

S. Minobe, Division of Earth and Planetary Sciences, Graduate School of Science, Hokkaido University, Sapporo 060-0810, Japan. (minobe@ep.sci.hokudai.ac.jp)

M. Nakamura, IBM Global Service Japan Solution and Services Company, Sapporo Center Buillding 21F, N-5, W-6, Sapporo 060-0005, Japan.